
Carina with HST

Star Cluster Formation in the Turbulent ISM

Ralf Klessen

Zentrum für Astronomie der Universität Heidelberg

Carina with HST

Star Cluster Formation in the Turbulent ISM

- ***importance of initial conditions:*** history matters!
- ***importance of dynamics:*** fragmentation induced starvation
- ***importance of geometry:*** interpreting line profiles

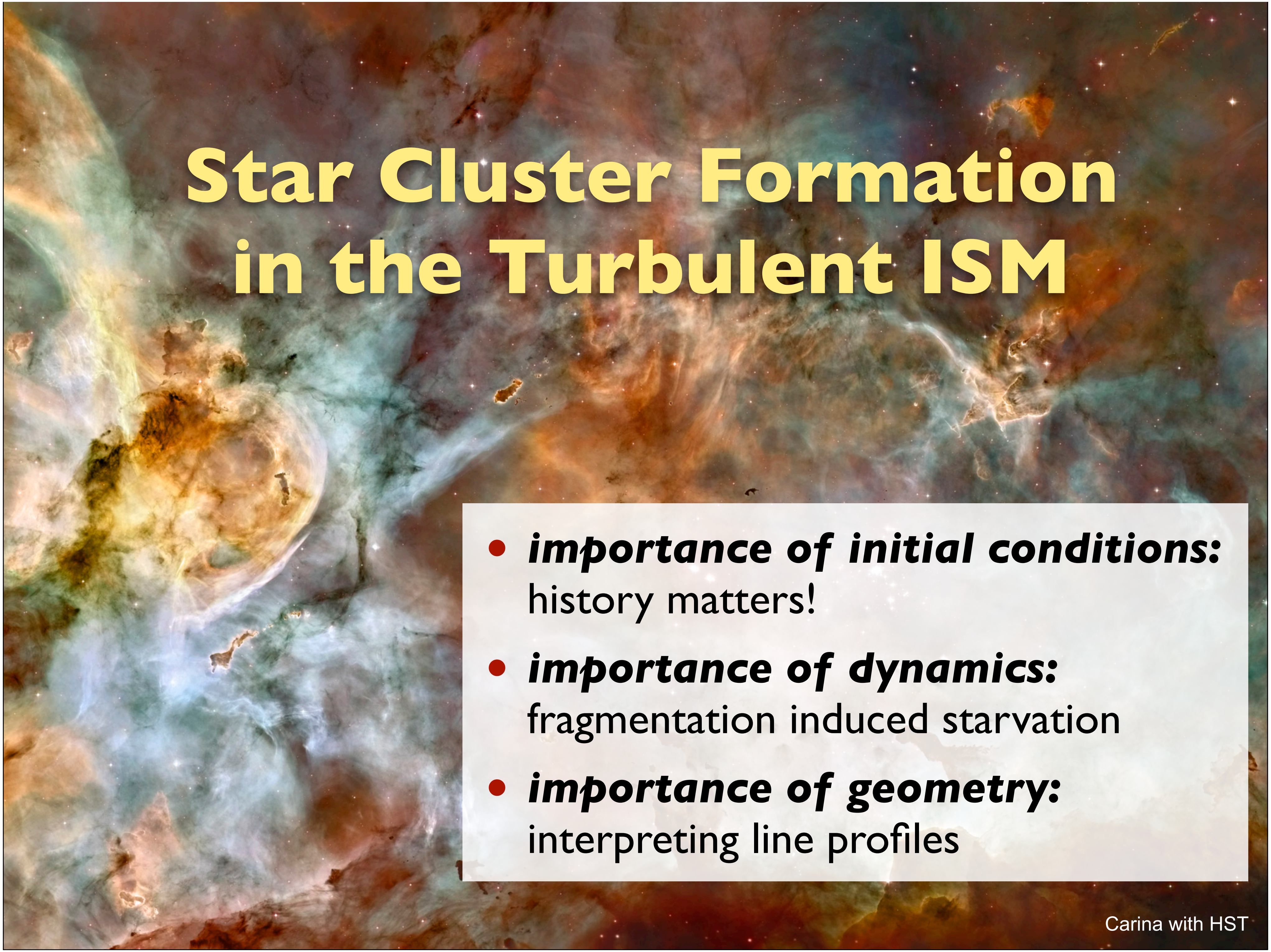

Carina with HST


DISCLAIMER
Carina with HST


Carina with HST

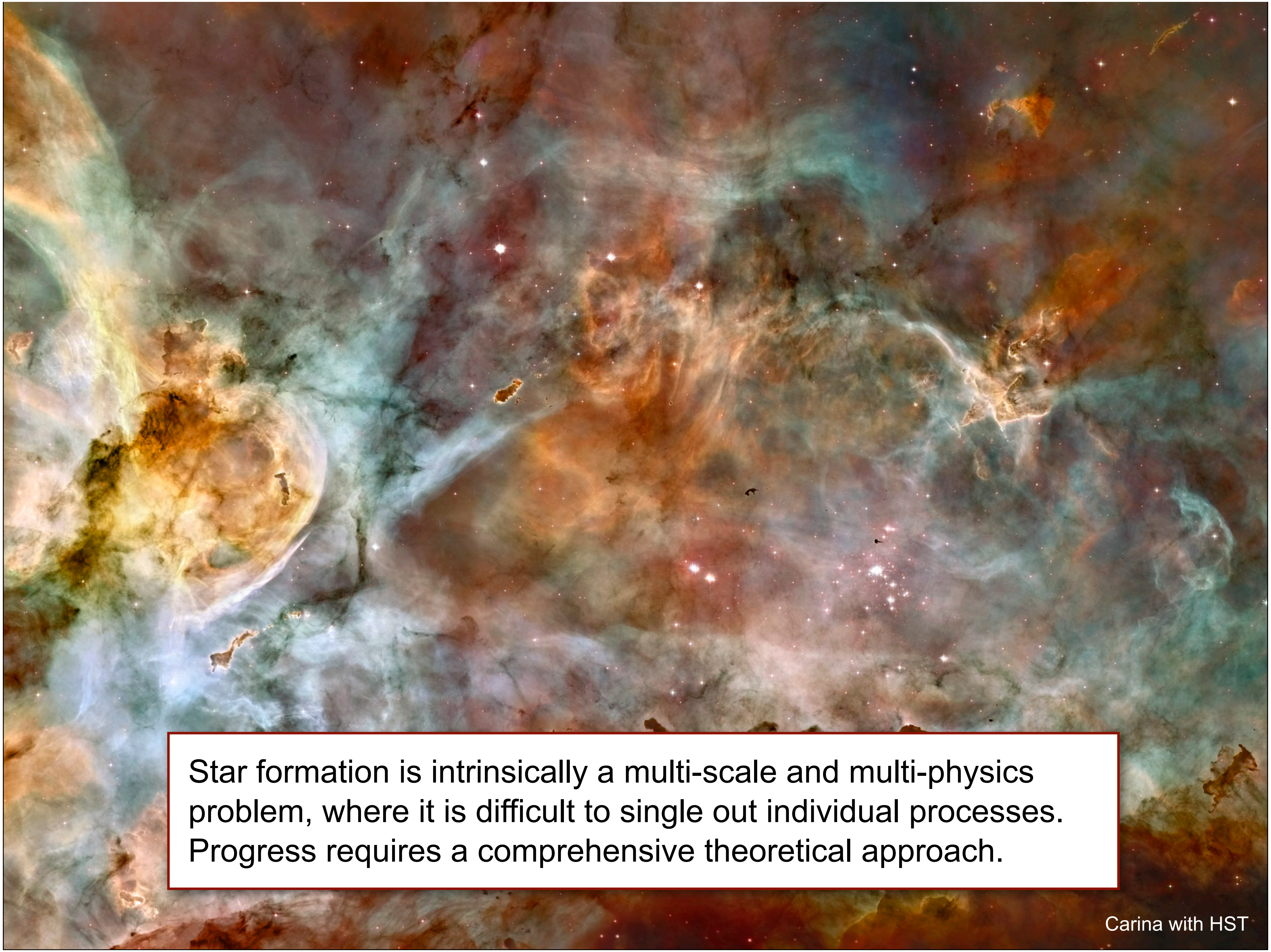

Star formation is intrinsically a multi-scale and multi-physics problem, where it is difficult to single out individual processes. Progress requires a comprehensive theoretical approach.

Carina with HST

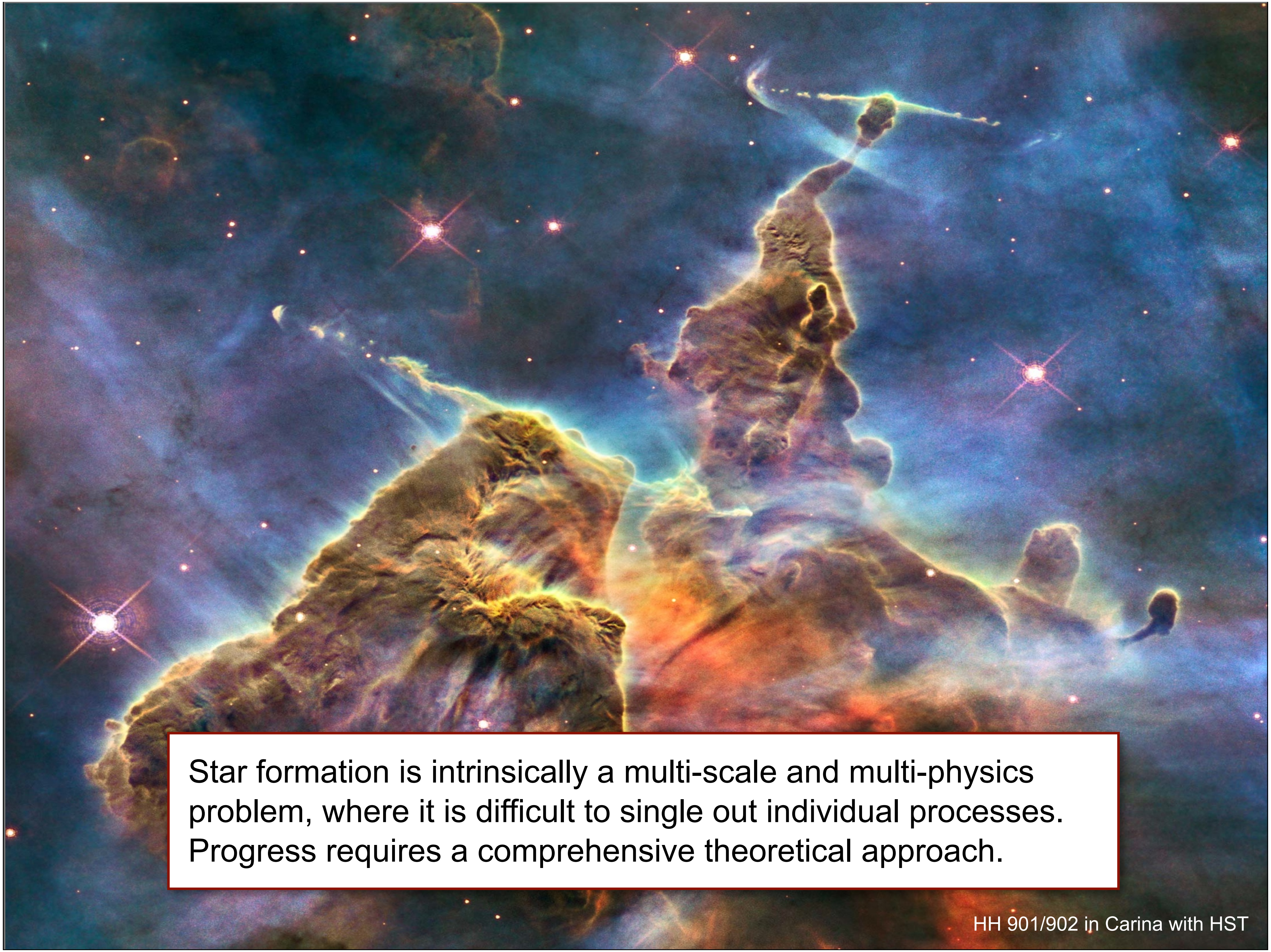

HH 901/902 in Carina with HST

selected open questions

- what processes determine the initial mass function (IMF) of stars?
- what are the initial conditions for star cluster formation?
  how does cloud structure translate into cluster structure?
- how do molecular clouds form and evolve?
- what drives turbulence?
- what triggers / regulates star formation on galactic scales?
- how does star formation depend on metallicity?
  how do the first stars form?
- star formation in extreme environments (galactic center, starburst, etc.),
  how does it differ from a more “normal” mode?

HH 901/902 in Carina with HST

selected open questions

- what processes determine the initial mass function (IMF) of stars?
- what are the initial conditions for star cluster formation?
  how does cloud structure translate into cluster structure?
- how do molecular clouds form and evolve?
- what drives turbulence?
- what triggers / regulates star formation on galactic scales?
- how does star formation depend on metallicity?
  how do the first stars form?
- star formation in extreme environments (galactic center, starburst, etc.),
  how does it differ from a more “normal” mode?

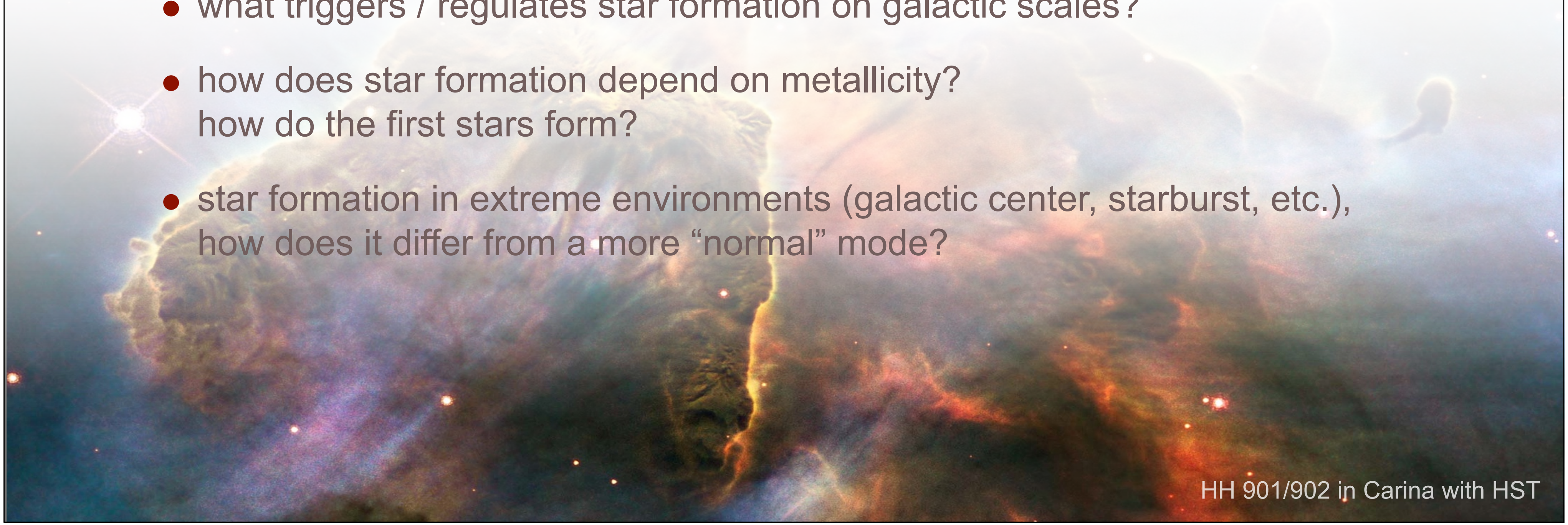

HH 901/902 in Carina with HST

stellar mass fuction

stars seem to follow a universal mass function at birth --> IMF

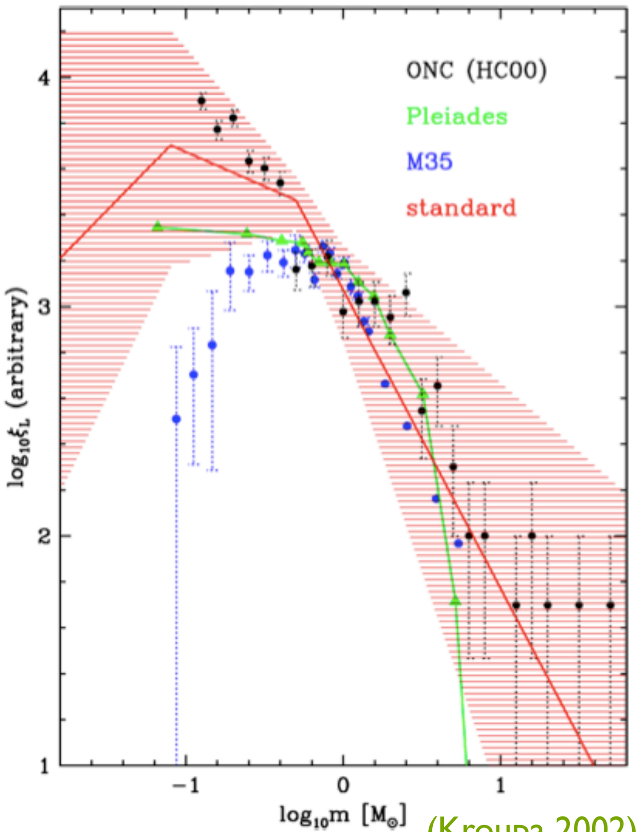

(Kroupa 2002)

Orion, NGC 3603, 30 Doradus
(Zinnecker & Yorke 2007)

stellar masses

- distribution of stellar masses depends on
  - turbulent initial conditions
    --> mass spectrum of prestellar cloud cores
  - collapse and interaction of prestellar cores
    --> accretion and *N*-body effects
  - thermodynamic properties of gas
    --> balance between heating and cooling
    --> EOS (determines which cores go into collapse)
  - (proto) stellar feedback terminates star formation
    ionizing radiation, bipolar outflows, winds, SN

(Kroupa 2002)

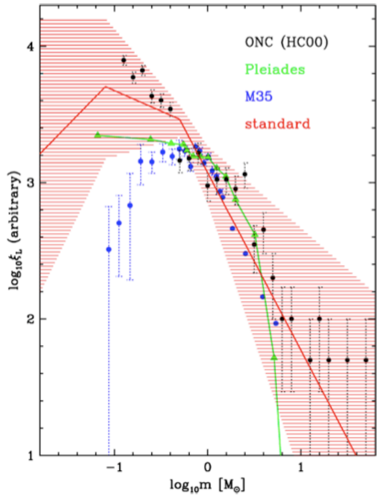

stellar masses

- distribution of stellar masses depends on
  - turbulent initial conditions
    --> mass spectrum of prestellar cloud cores
  - collapse and interaction of prestellar cores
    --> accretion and *N*-body effects
  - thermodynamic properties of gas
    --> balance between heating and cooling
    --> EOS (determines which cores go into collapse)
  - (proto) stellar feedback terminates star formation
    ionizing radiation, bipolar outflows, winds, SN

(Kroupa 2002)

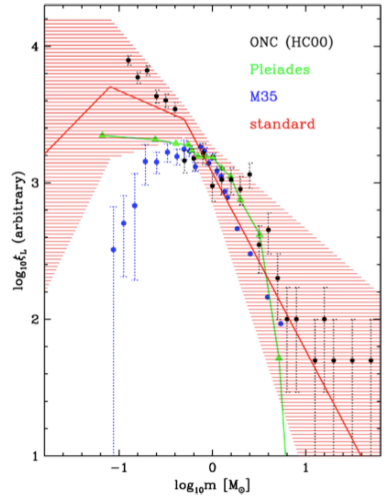

example: model of Orion cloud

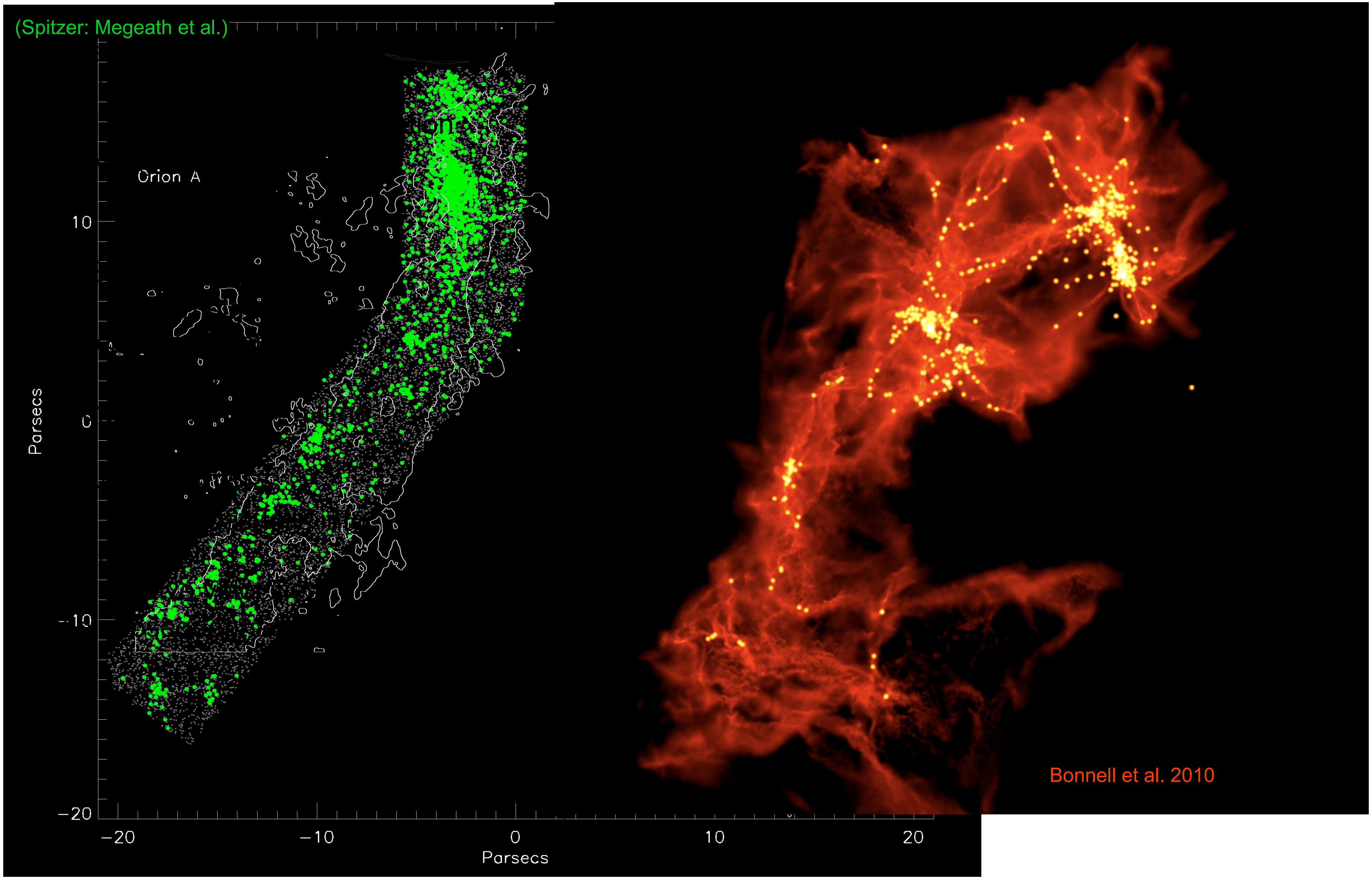

Dynamics of nascent star cluster

in dense clusters protostellar interaction may be come important!

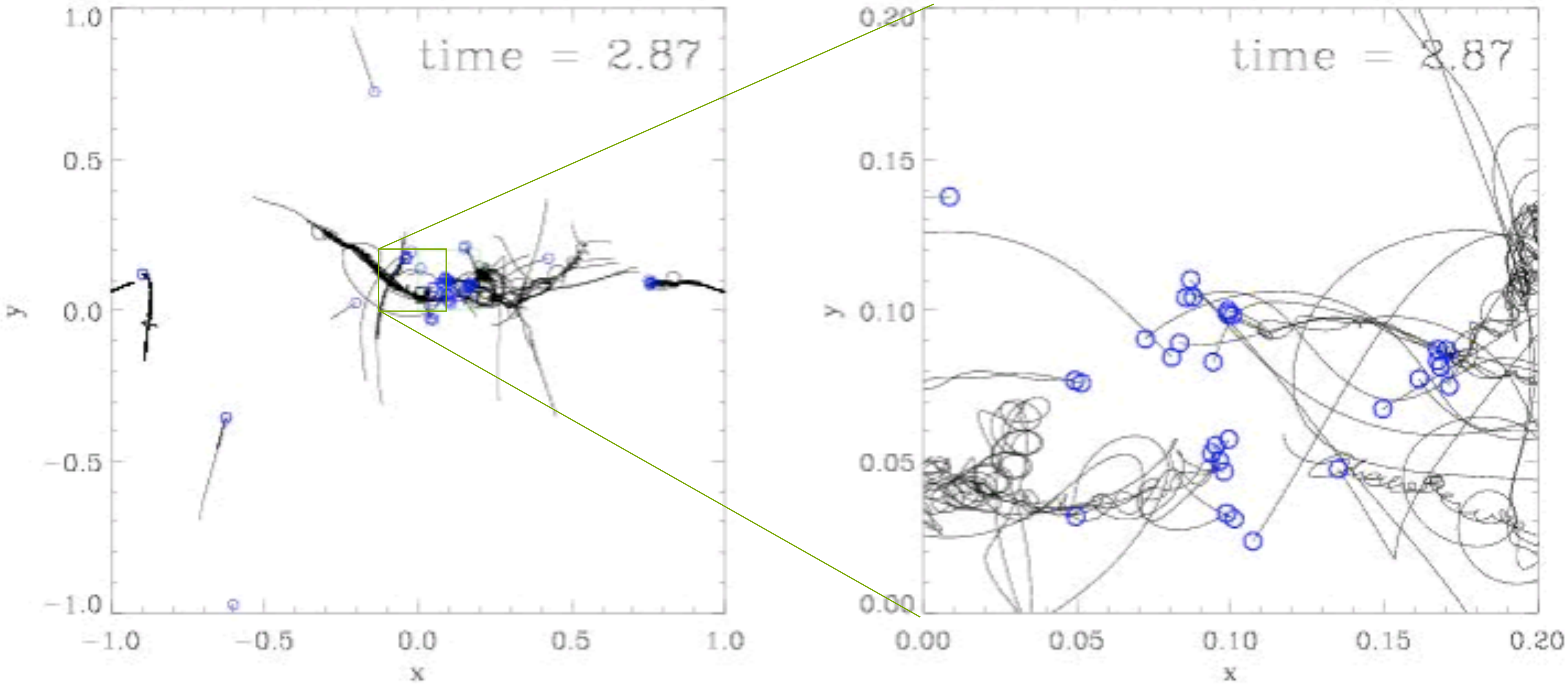

Trajectories of protostars in a nascent dense cluster created by gravoturbulent fragmentation
(from Klessen & Burkert 2000, ApJS, 128, 287)

accretion rates in clust

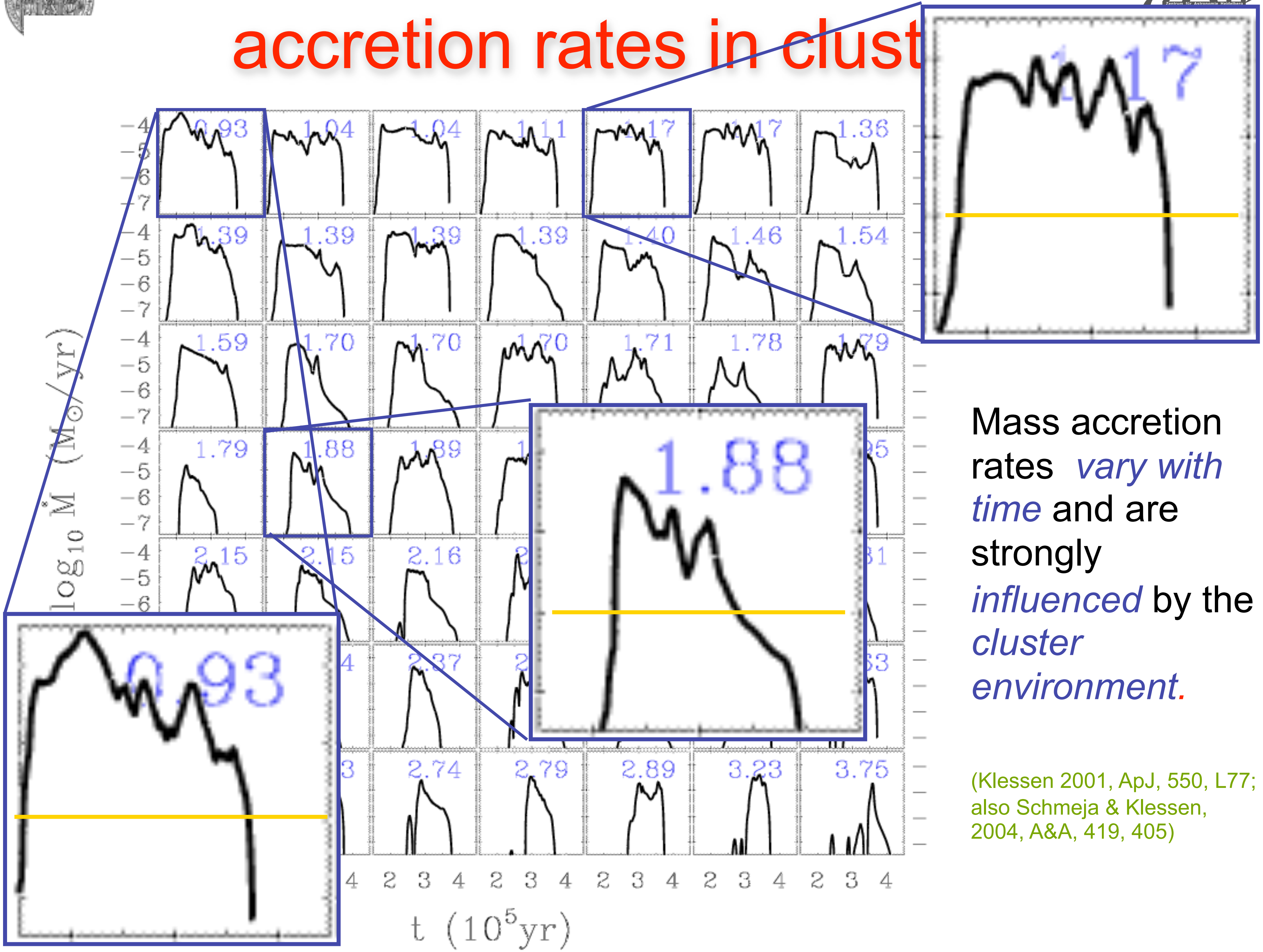

Mass accretion rates *vary with time* and are strongly *influenced* by the *cluster environment*.

(Klessen 2001, ApJ, 550, L77; also Schmeja & Klessen, 2004, A&A, 419, 405) importance of initial conditions

ICs of star cluster formation

- key question:
  - what is the initial density profile of cluster forming cores? how does it compare low-mass cores?
- observers answer:
  - very difficult to determine!
    - most high-mass cores have some SF inside
    - infra-red dark clouds (IRDCs) are difficult to study
  - but: new results with Herschel

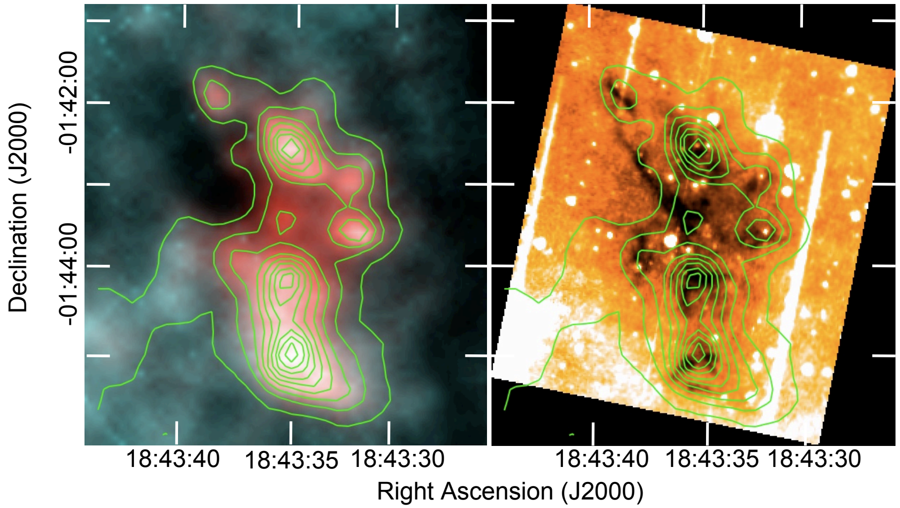

IRDC observed with Herschel, Peretto et al. (2010)

different density profiles

- key question:
  - what is the initial density profile of cluster forming cores? how does it compare low-mass cores?
- theorists answer:
  - top hat (Larson Penston)
  - Bonnor Ebert (like low-mass cores)
  - power law $\rho \propto r^{-1}$ (logotrop)
  - power law $\rho \propto r^{-3/2}$ (Krumholz, McKee, et
  - power law $\rho \propto r^{-2}$ (Shu)
  - and many more

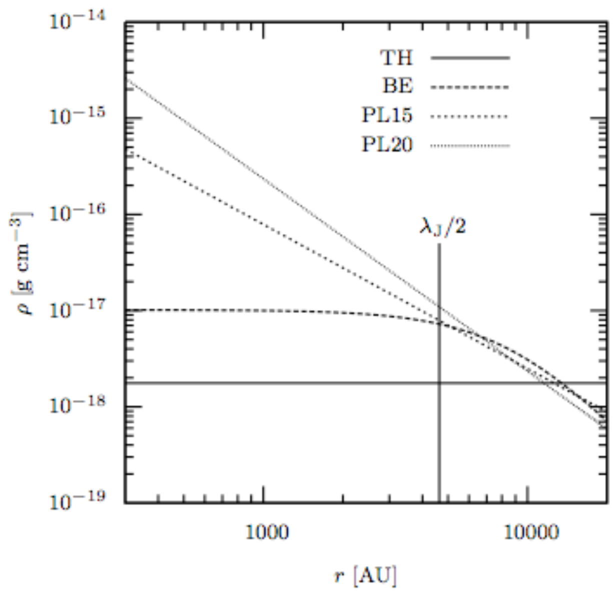

different density profiles

- does the density profile matter?

  .

  .

  .

- in comparison to
  - turbulence ...
  - radiative feedback ...
  - magnetic fields ...
  - thermodynamics ...

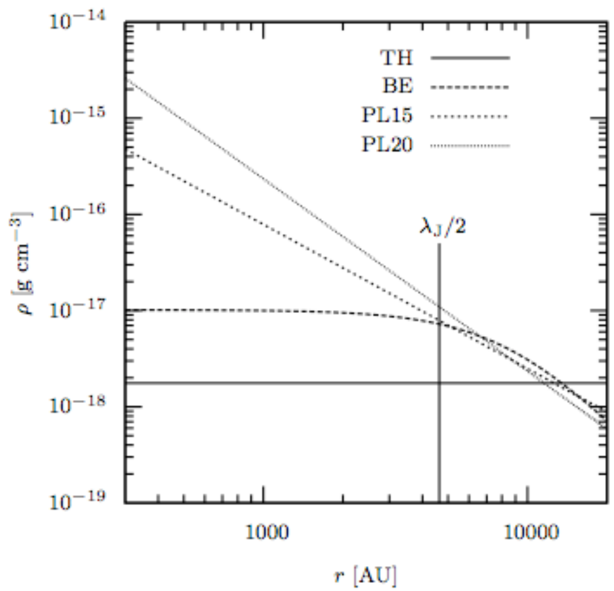

different density profiles

- address question in simple numerical experiment
- perform extensive parameter study
  - different profiles (top hat, BE, $r^{-3/2}$, r^{-3})
  - different turbulence fields
    - different realizations
    - different Mach numbers
    - solenoidal turbulence
dilatational turbulence
both modes
  - no net rotation, no B-fields
(at the moment)

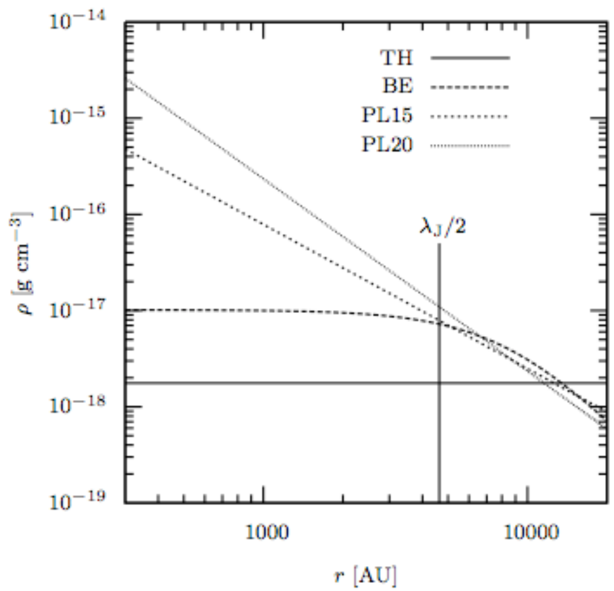

Girichids, Federrath, Banerjee, Klessen (2011abc)

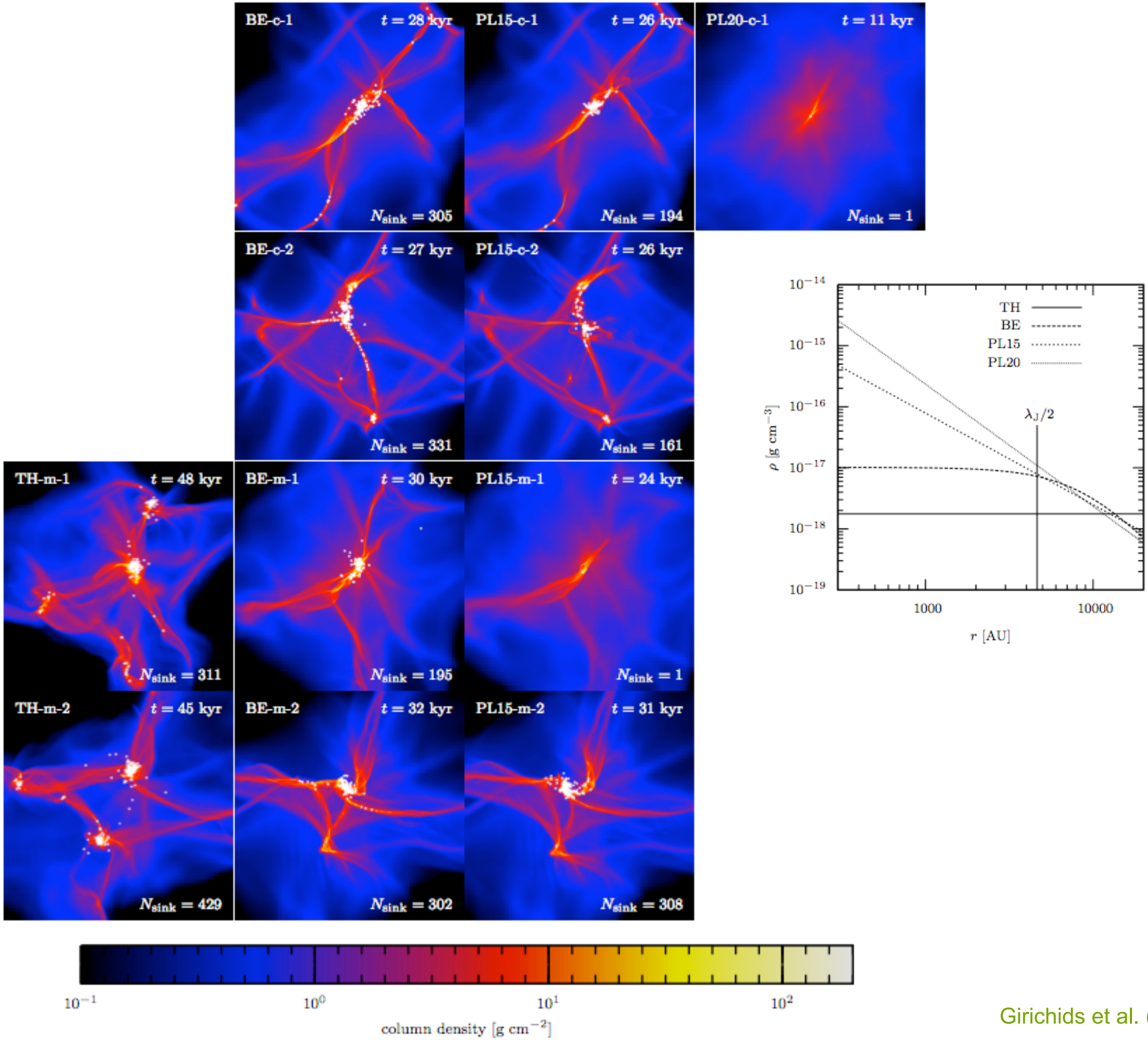

Girichids et al. (2011abc)

Run	t_{sim} [kyr]	t_{sim}/t_{ff}^{core}	t_{sim}/t_{ff}	N_{sinks}	$\langle M \rangle$ [$M_{\odot}$]	M_{max}
TH-m-1	48.01	0.96	0.96	311	0.0634	0.86
TH-m-2	45.46	0.91	0.91	429	0.0461	0.74
BE-c-1	27.52	1.19	0.55	305	0.0595	0.94
BE-c-2	27.49	1.19	0.55	331	0.0571	0.97
BE-m-1	30.05	1.30	0.60	195	0.0873	1.42
BE-m-2	31.94	1.39	0.64	302	0.0616	0.54
BE-s-1	30.93	1.34	0.62	234	0.0775	1.14
BE-s-2	35.86	1.55	0.72	325	0.0587	0.51
PL15-c-1	25.67	1.54	0.51	194	0.0992	8.89
PL15-c-2	25.82	1.55	0.52	161	0.1244	12.3
PL15-m-1	23.77	1.42	0.48	1	20	20.0
PL15-m-2	31.10	1.86	0.62	308	0.0653	6.88
PL15-s-1	24.85	1.49	0.50	1	20	20.0
PL15-s-2	35.96	2.10	0.72	422	0.0478	4.50
PL20-c-1	10.67	0.92	0.21	1	20	20.0

number of protostars

ICs with flat inner density profile on average form more fragments

Girichids et al. (2011abc)

Run	t_{sim} [kyr]	t_{sim}/t_{ff}^{core}	t_{sim}/t_{ff}	N_{sinks}	$\langle M \rangle$ [$M_\odot$]	M_{max}
TH-m-1	48.01	0.96	0.96	311	0.0634	0.86
TH-m-2	45.46	0.91	0.91	429	0.0461	0.74
BE-c-1	27.52	1.19	0.55	305	0.0595	0.94
BE-c-2	27.49	1.19	0.55	331	0.0571	0.97
BE-m-1	30.05	1.30	0.60	195	0.0873	1.42
BE-m-2	31.94	1.39	0.64	302	0.0616	0.54
BE-s-1	30.93	1.34	0.62	234	0.0775	1.14
BE-s-2	35.86	1.55	0.72	325	0.0587	0.51
PL15-c-1	25.67	1.54	0.51	194	0.0992	8.89
PL15-c-2	25.82	1.55	0.52	161	0.1244	12.3
PL15-m-1	23.77	1.42	0.48	1	20	20.0
PL15-m-2	31.10	1.86	0.62	308	0.0653	6.88
PL15-s-1	24.85	1.49	0.50	1	20	20.0
PL15-s-2	35.96	2.10	0.72	422	0.0478	4.50
PL20-c-1	10.67	0.92	0.21	1	20	20.0

number of protostars

ICs with flat inner density profile on average form more fragments

however, the real situation is very complex: details of the initial turbulent field matter

different density profiles

- different density profiles lead to very different fragmentation behavior
- fragmentation is strongly suppressed for very peaked, power-law profiles
- this is *good* because it may explain some of the theoretical controversy, we have in the field
- this is *bad*, because all current calculations are "wrong" in the sense that the formation process of the star-forming core is neglected.
- *CONCLUSION:* take molecular cloud formation into account in theoretical / numerical models!

stellar mass fuction

- distribution of stellar masses depends on
  - turbulent initial conditions
    --> mass spectrum of prestellar cloud cores
  - collapse and interaction of prestellar cores
    --> accretion and *N*-body effects
  - thermodynamic properties of gas
    --> balance between heating and cooling
    --> EOS (determines which cores go into collapse)
  - (proto) stellar feedback terminates star formation
    ionizing radiation, bipolar outflows, winds, SN, etc.

(Kroupa 2002)

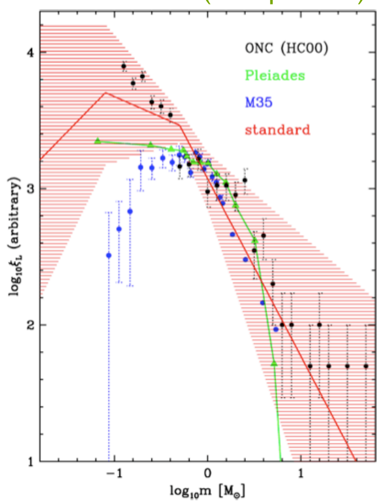

stellar masses

- distribution of stellar masses depends on
  - turbulent initial conditions
    --> mass spectrum of prestellar cloud cores
  - collapse and interaction of prestellar cores
    --> accretion and *N*-body effects
  - thermodynamic properties of gas
    --> balance between heating and cooling
    --> EOS (determines which cores go into collapse)
  - (proto) stellar feedback terminates star formation
    ionizing radiation, bipolar outflows, winds, SN

(Kroupa 2002)

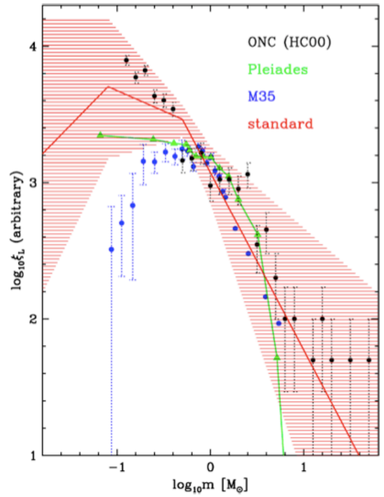

Importance of dynamics

SKIPPED IN TALK

importance of geometry

line profiles

- key question:
  - what can we learn from line profiles about the dynamic state of prestellar cores?
  - what are the best tracers?

Smith et al. (2012, ApJ, 750, 64), Smith et al. (2013, ApJ, 771, 24), Chira et al. (in preparation)

line profiles

- key question:
  - what can we learn from line profiles about the dynamic state of prestellar cores?
  - what are the best tracers?

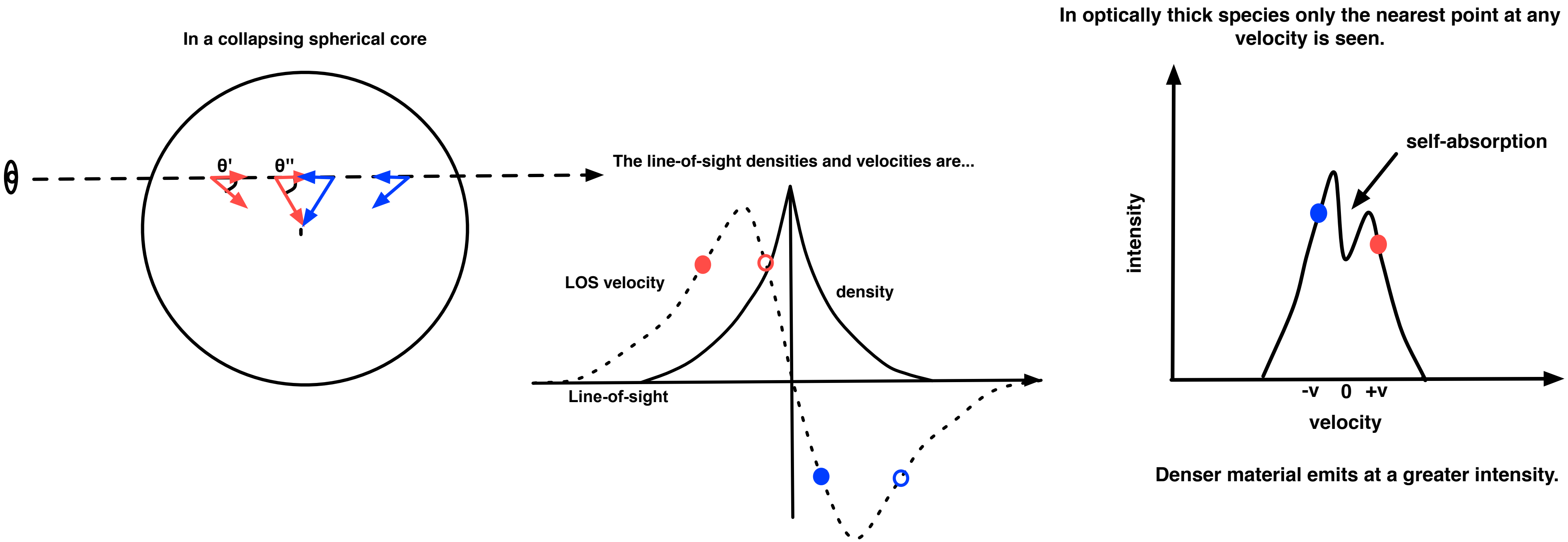

Smith et al. (2012, ApJ, 750, 64), Smith et al. (2013, ApJ, 771, 24), Chira et al. (in preparation)

line profiles

- key question:
  - what can we learn from line profiles about the dynamic state of prestellar cores?
  - what are the best tracers?

Tracer	Transition Line	Critical Density n_{crit}	Optically
		cm^{-3}	
N_2H^+	J = (1-0)[2], (3-2)	1.6×10^5, 3.0×10^6	thin
^{13}CO	J = (3-2)	1.9×10^3	thin
$H^{13}CO^+$	J = (3-2)	1.7×10^5	thin
HCN	J = (1-0) – (5-4)[3]	1.0×10^6 – 9.7×10^8	thick
HCO^+	J = (1-0) – (5-4)[3]	1.6×10^5 – 1.7×10^7	thick
CS	J = (1-0) – (5-4)[3]	4.7×10^5 – 8.1×10^6	thick

Smith et al. (2012, ApJ, 750, 64), Smith et al. (2013, ApJ, 771, 24), Chira et al. (in preparation)

core A

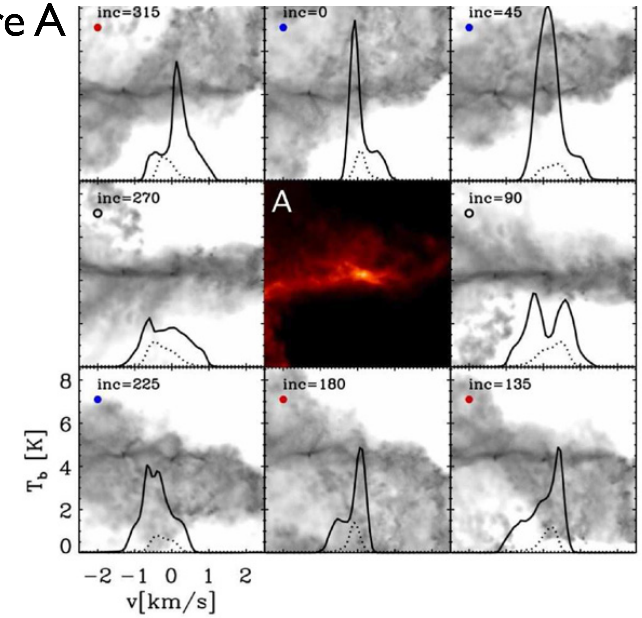

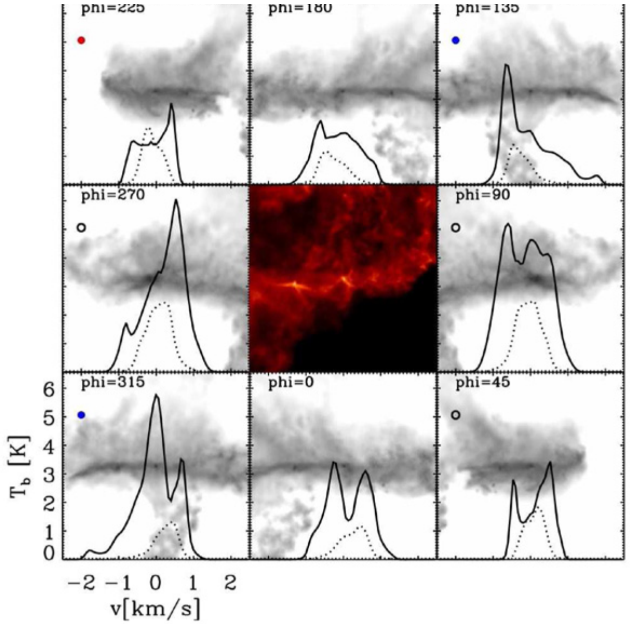

opt. thick tracer
HCN F(2-1)

opt. thin tracer
H_2H^+ (1-0)

core B

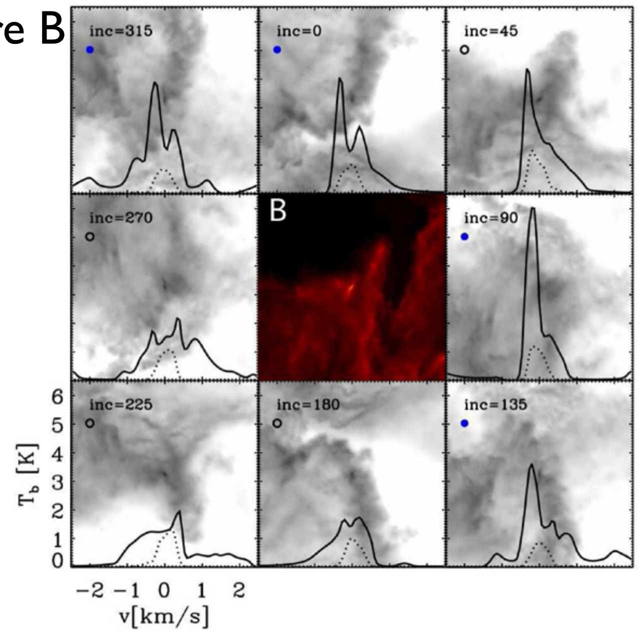

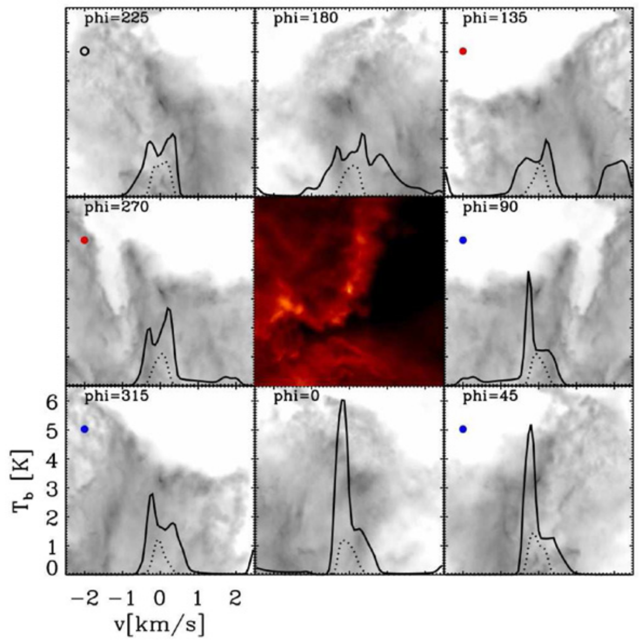

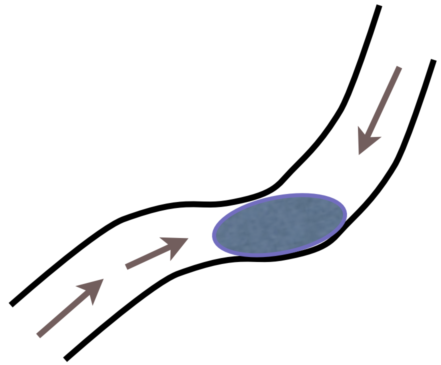

collapsing prestellar core embedded in filamentary structure

seen at different viewing angles

Smith et al. (2012, ApJ, 750, 64), Smith et al. (2013, ApJ, 771, 24), Chira et al. (in preparation)

results

A Summary of the Classification Types Assigned to the HCN F(2–1) Lines from Filaments A, B, and C using the Line Profile Shapes

Filament	Blue	Red	Ambiguous
A	5/14	4/14	5/14
B	7/14	2/14	5/14
C	3/14	1/14	10/14
Total	15/42	7/42	20/42
	36%	17%	47%

Note. Despite the fact that the embedded cores are collapsing, a blue asymmetric line profile is seen in only 36% of cases.

Smith et al. (2012, ApJ, 750, 64), Smith et al. (2013, ApJ, 771, 24), Chira et al. (in preparation)

result depends on transition

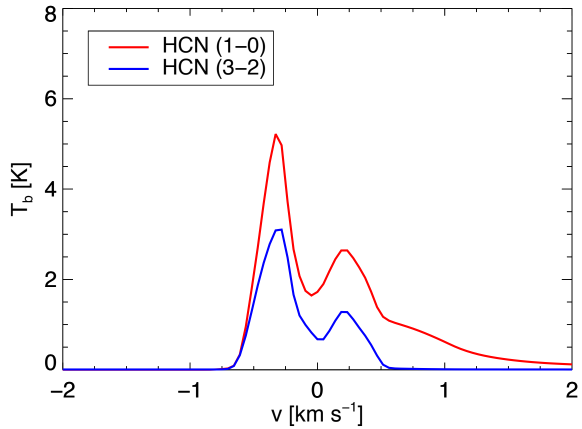

both transitions show
BLUE assymmetry

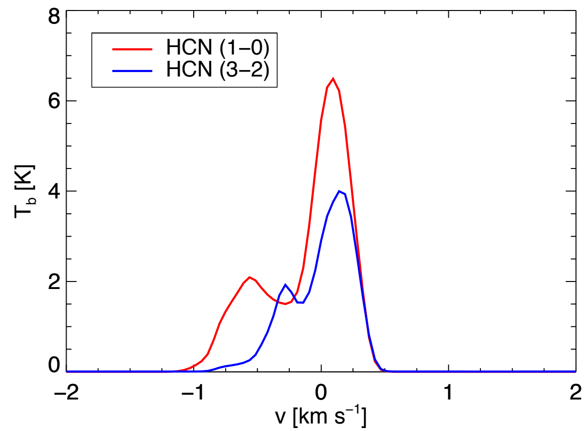

both transitions show
RED assymmetry

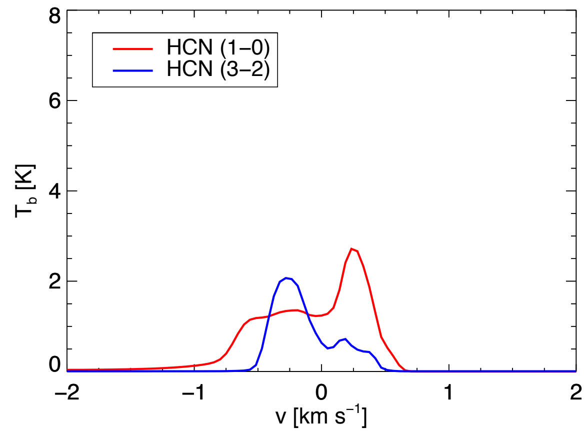

both transitions show
DIFFERENT assymmetry

HCN

Smith et al. (2012, ApJ, 750, 64), Smith et al. (2013, ApJ, 771, 24), Chira et al. (in preparation)

result depends on transition

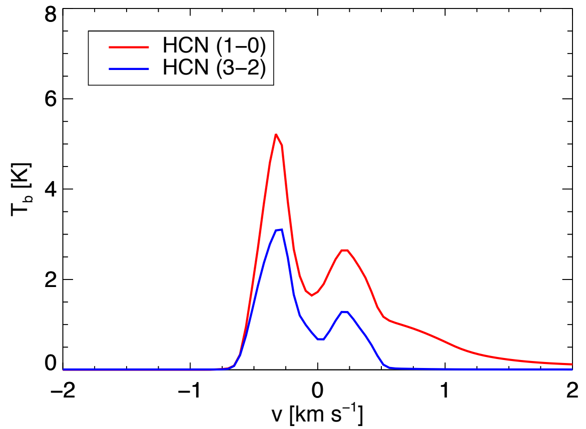

both transitions show
BLUE assymmetry

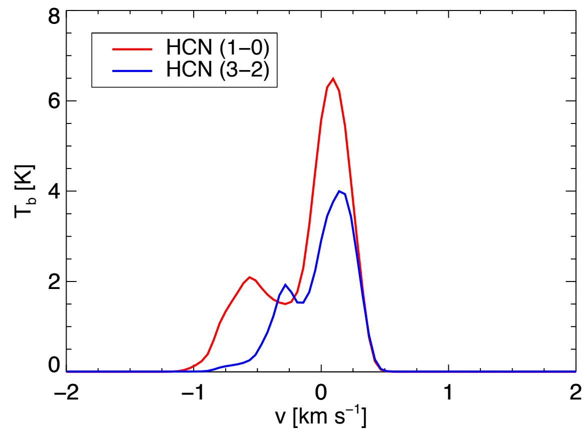

both transitions show
RED assymmetry

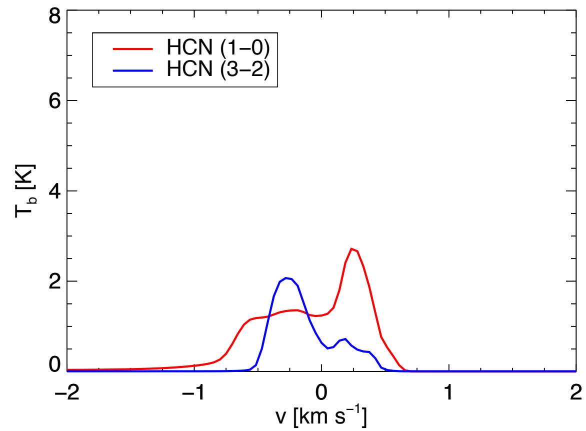

both transitions show
DIFFERENT assymmetry

HCN

Smith et al. (2012, ApJ, 750, 64), Smith et al. (2013, ApJ, 771, 24), Chira et al. (in preparation)

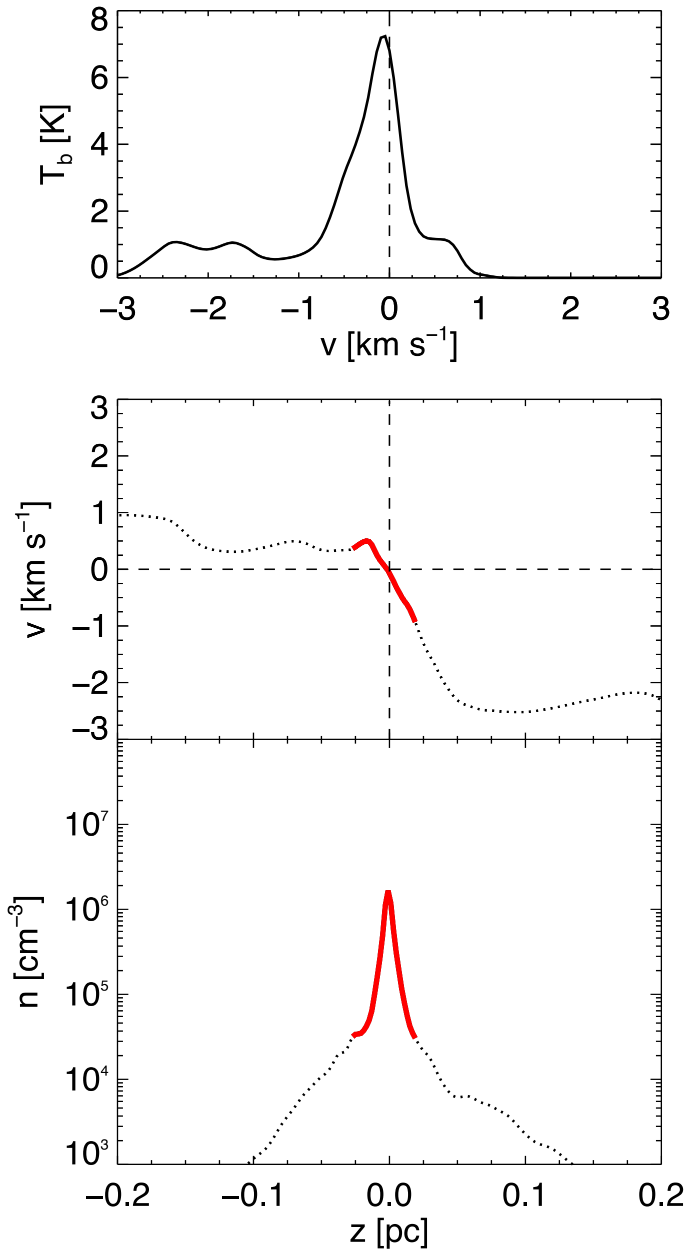

looking at the velocity and density along the line of sight, we can understand the resulting line profile

Figure 3.3: *upper panel:* Line profile of HCN (1-0) observed in Core C at $i = 0°$ and $\phi = 0°$. *lower panel:* n - v - Diagram of Core C at $i = 0°$ and $\phi = 0°$. The number density and velocity distribution are plotted with dashed lines. Thick black lines mark regions with number densities higher than 3×10^4 cm^{-3}, red lines mark areas within a radius of 0.05 pc around the core centre. One sees that the origin of the line profile component arounf 0 km s^{-1} can be associated with the central core region where number density is highest. The second component belongs to the density bump at $z = 0.07$ pc.

Smith et al. (2012, ApJ, 750, 64),
Smith et al. (2013, ApJ, 771, 24),
Chira et al. (in preparation)

HCN

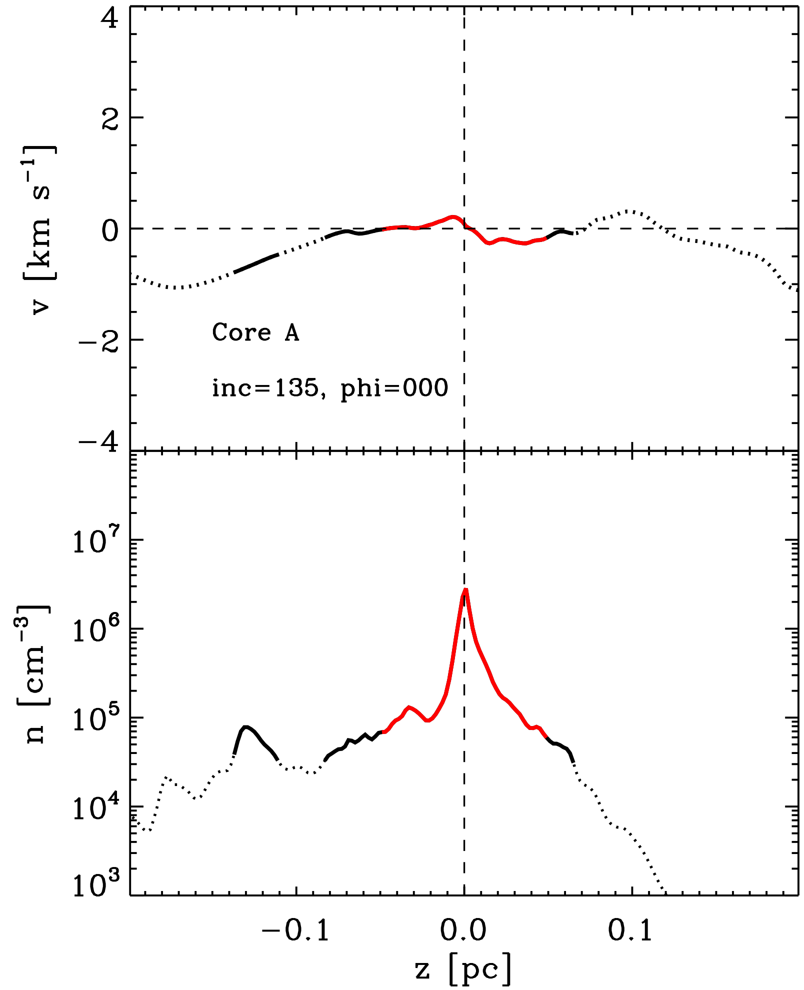

Figure A.14: $n - v$ – diagram of Core A at $i = 135°$ and $\phi = 0°$. As in Fig. A.13.

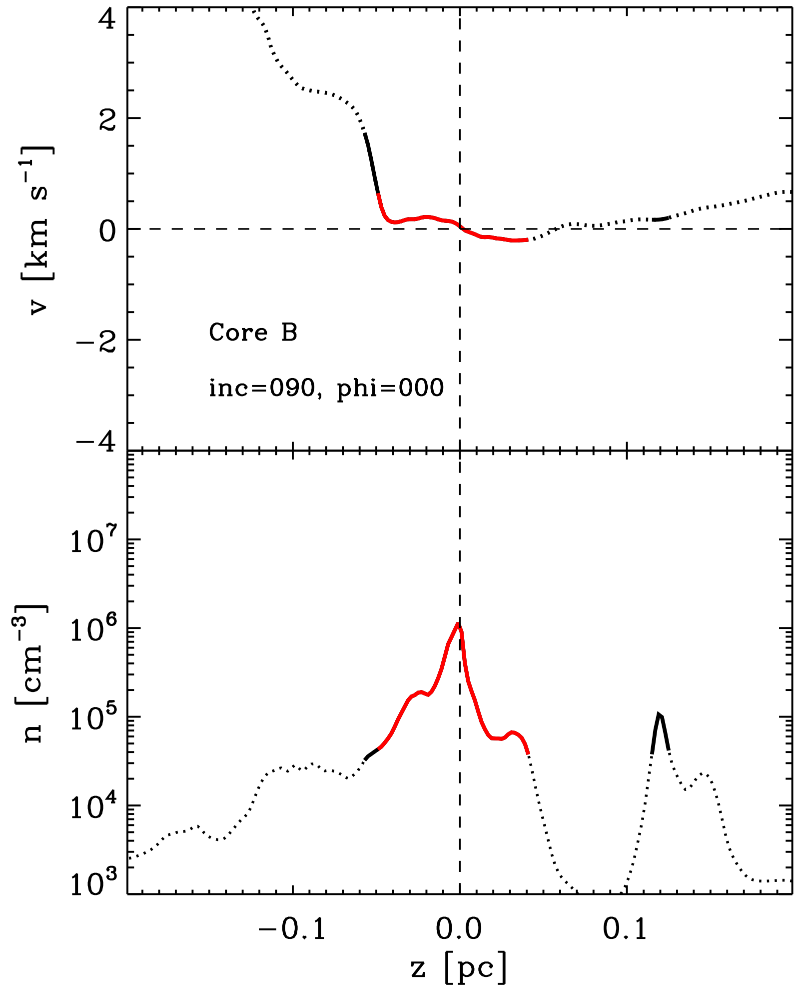

Figure A.13: $n - v$ – diagram of Core B at $i = 90°$ and $\phi = 0°$. The number density and velocity distribution are plotted with dashed lines. Thick black lines mark regions with number densities higher than 3×10^4 cm^{-3}, red lines such within a radius of 0.05 pc around the core centre.

HCN

Smith et al. (2012, ApJ, 750, 64), Smith et al. (2013, ApJ, 771, 24), Chira et al. (in preparation)

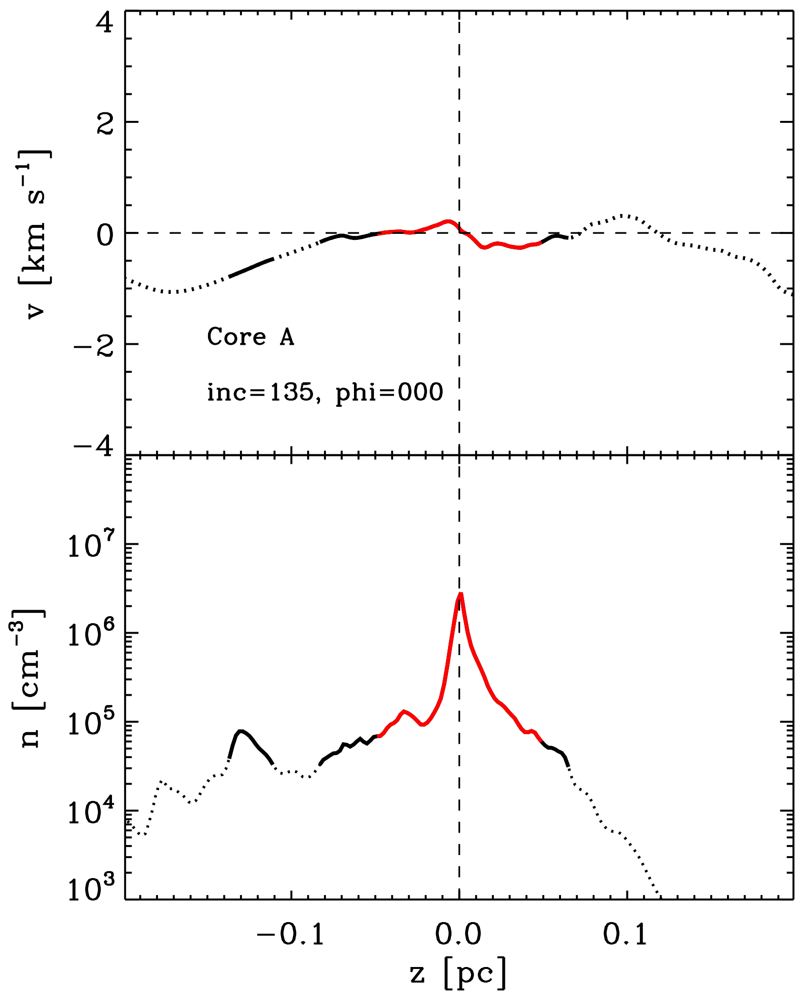

Figure A.14: $n - v$ – diagram of Core A at $i = 135°$ and $\phi = 0°$. As in Fig. A.13.

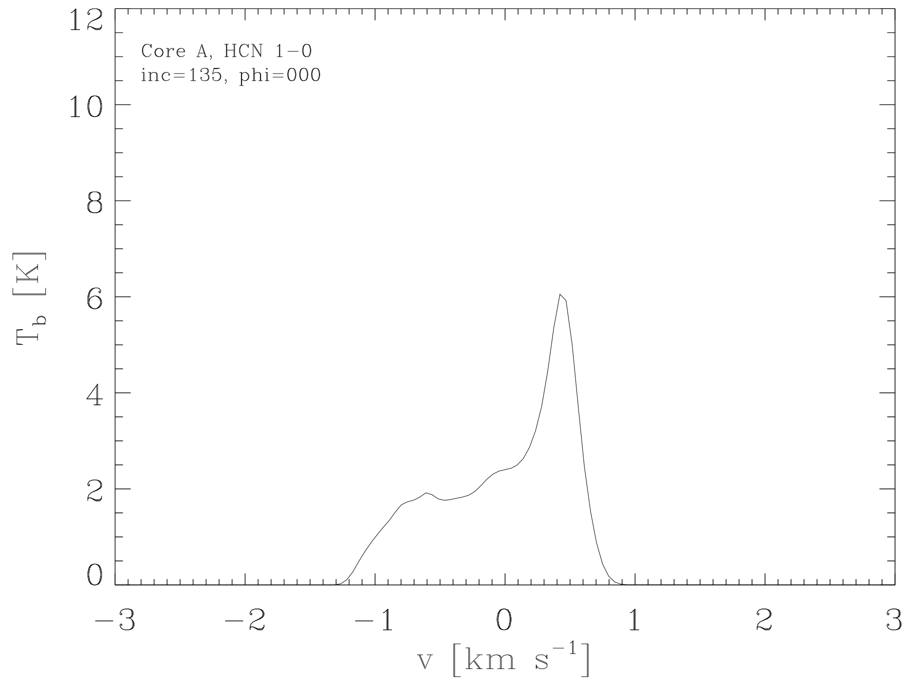

Figure A.15: Red asymmetric line profile of HCN (1-0) in Core A at $i = 135°$ and $\phi = 0°$.

RED **profile despite collapse**

HCN

Smith et al. (2012, ApJ, 750, 64), Smith et al. (2013, ApJ, 771, 24), Chira et al. (in preparation)

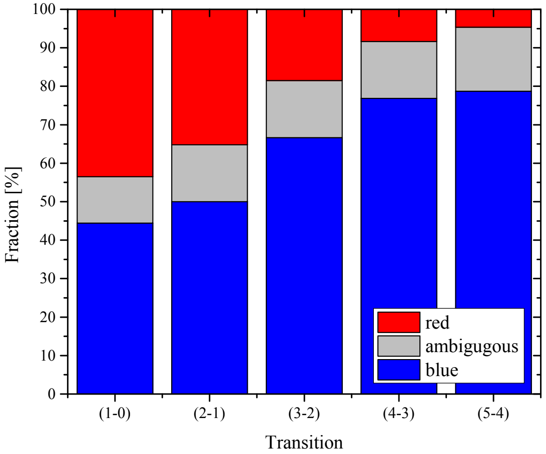

(a) N_2H^+ (1-0)

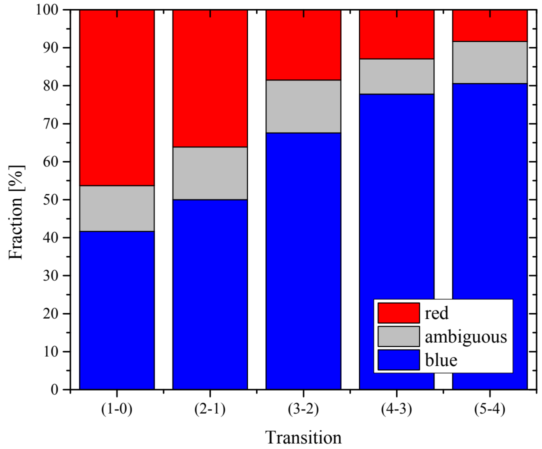

(b) N_2H^+ (3-2)

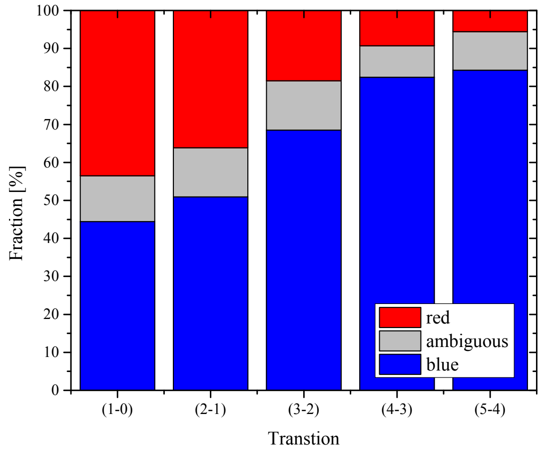

(c) $H^{13}CO^+$ (3-2)

HCN with N_2H^+ (1-0) as reference line

HCN with N_2H^+ (3-2) as reference line

HCN with $H^{13}CO^+$ (3-2) as reference line

The "higher" the transition, the better the classification.
BUT: The "higher" the transition, the weaker the signal

CONCLUSION: The best tracer of our sample is the (4-3) transition of HCN, but the (3-2) and (5-4) transitions also okay.

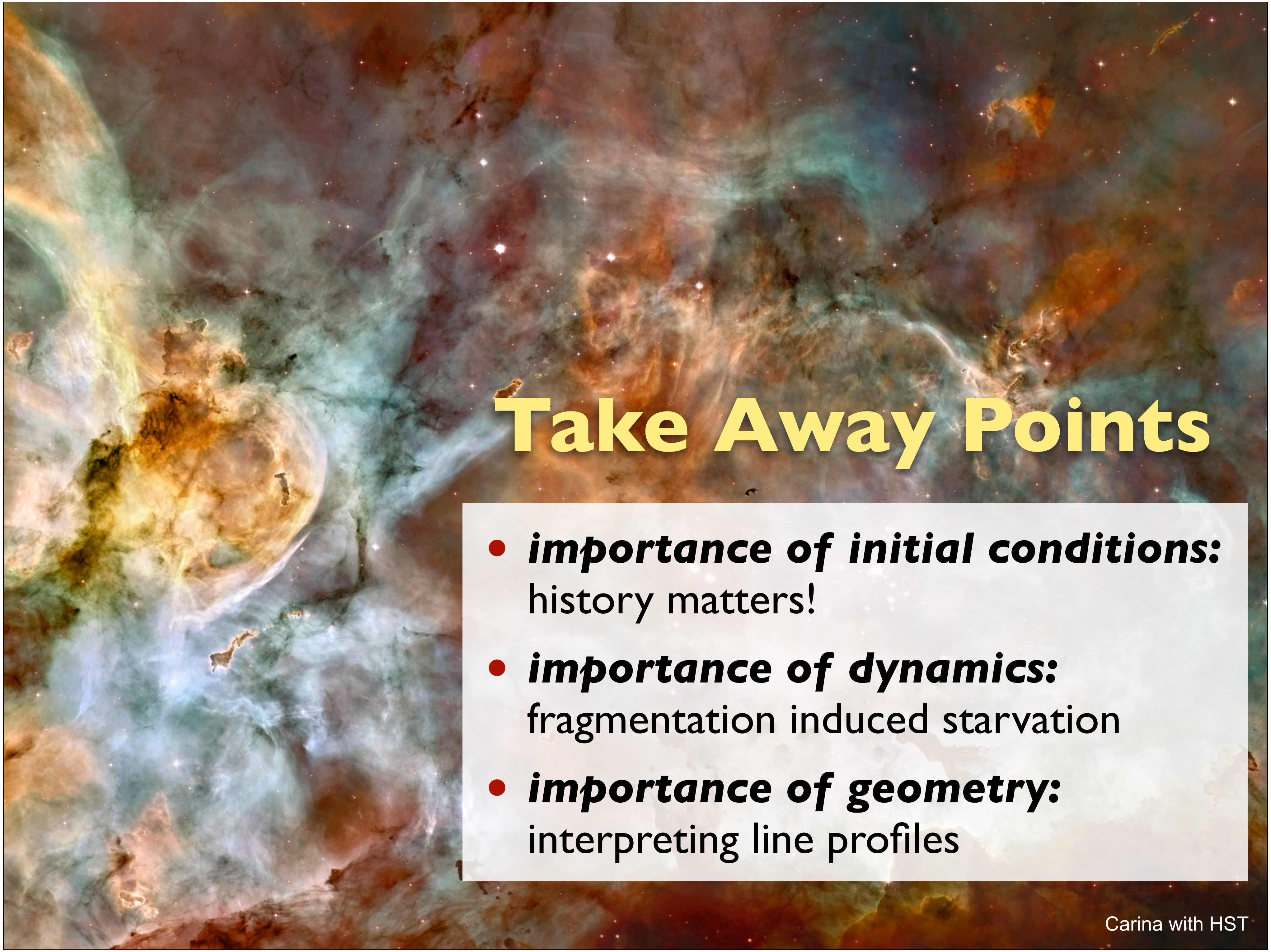
Take Away Points
• importance of initial conditions: history matters!
• importance of dynamics: fragmentation induced starvation
• importance of geometry: interpreting line profiles
Carina with HST